JOURNAL OF THE BALKAN GEOPHYSICAL SOCIETY, Vol. 6, No. 2, May 2003, p. 53 – 65, 10 figs.

Relationships among source parameters of aftershocks of the October 1, 1995 Dinar (Turkey) earthquake

E. Yalçýnkaya* and Ö. Alptekin*

*Istanbul University, Department of Geophysical Engineering, 34850 Avcýlar, Istanbul, Turkey.
e-mail: eyalcin@istanbul.edu.tr

(Received 29 October 2002; accepted 28 January 2003)

Abstract: *We estimated the source parameters of 53 aftershocks (2.5 £ M_L £ 4.1) of the October 1, 1995 Dinar earthquake in southwestern Turkey. Focal depths and hypocentral distances of the aftershocks range from 5 km to 15 km and 6 km to 30 km respectively, and a circular source model (Brune, 1970) is used in the analysis of S-wave displacement spectra. Although it was a moderately strong earthquake (M_L = 6.0, M_W = 6.2) the main shock and its moderately strong aftershocks perished nearly 90 people and damaged about 4500 buildings, mainly because of poor ground conditions. Our study revealed that the seismic moment, source radius, and stress drop of the aftershocks range in the following intervals: 7.35E+19 £ M_0 £ 3.35E+22 dyne.cm, 0.15 £ r £ 0.57 km, 5.13 £ Ds £ 100.09 bars respectively. For earthquakes of M_0 < 1.0E+21 dyne.cm the corner frequency does not increase with decreasing seismic moment, and the stress drop shows a step near to M_0 » 1.0E+21 dyne.cm. The spectra have been affected from the attenuation only at high frequencies. The S-wave spectra have been significantly affected from the soil conditions underlying the receivers.*

Key words: *Source parameters, Dinar earthquake, Attenuation, Site effect*

INTRODUCTION

Source parameters like the seismic moment, stress drop, and source radius of earthquakes for different parts of the world have been investigated by Aki (1967), Brune (1970), Hanks and Kanamori (1979), Ishida and Kanamori (1980), Fletcher (1980). These studies have shown the importance of source parameters and the relationships among them not only towards understanding the kinematical and dynamical properties of earthquake source, but also understanding the seismotectonics of an area (Mandal *et al.*, 1998).

The results indicated that the stress drop is nearly constant, independent of earthquake size (Kanamori and Anderson, 1975). In other words, the shape of source spectrum changes with the size following a scaling relation as predicted by Aki (1967). The removal of the path and site effects in estimating the source parameters of small earthquakes is an important but still an unsolved problem. An attenuation study for each studied area is necessary but not available in most cases. Nevertheless, spectra of small earthquakes have been interpreted using simple models such as the circular crack model developed by Brune (1970). Many previous investigations found that the corner frequency of small events increase very slowly or become constant with decreasing seismic moment below a certain value, implying a breakdown in the self-similarity of the rupture processes for small earthquakes (e.g. Chouet et al., 1978; Rautian et al., 1978; Archuleta et al., 1982; Hanks, 1982). Later studies concluded that the apparent high-frequency limit to corner frequency may be mainly due to high attenuation in the weathered, near surface material (Andrews, 1982; Frankel and Wennerberg, 1989).

The number of studies on the source parameters of Turkish earthquakes is very limited. Polat (1995), Biçmen (1992) have used the Brune's model to estimate the source parameters of local earthquakes in the Marmara region. Kaypak (1995) has used the Brune's model to estimate the source parameters and the relations among them for aftershocks of the March 13, 1992 Erzincan earthquake.

The first aim of this study is to estimate source parameters and relationships among them by using the 53 aftershock records of the October 1, 1995 Dinar earthquake. The second aim is to investigate the effects of attenuation and local soil conditions on the spectral characteristics of seismograms recorded on different soil conditions.

DATA

A moderately strong earthquake (M_L = 6.0, M_W = 6.2) occurred close to the town of Dinar at 15:57 UT on October 1, 1995 killing 90 people and damaging about 4500 buildings. The epicenter coordinates of the earthquake were given as 38.06° N and 30.13° E by USGS, being close to the Dinar-Çivril fault. The earthquake was associated with two subevents (Utkucu *et al.*, 2002). Surface cracks have been observed 10 km continuously along the Dinar-Çivril fault (Öncel *et al.*, 1998). The west block of this fault is a graben (Dinar Graben) while the east block represents a horst (Akdað Horst) (Koçyiðit, 1984). The graben so called the alluvial zone in Figure 1 has been filled with very young (Plio-Quaternary age) and fairly thick (30-80 m) unconsolidated sediments (pebbles, sand, silt and clay). The horst so called the mountain zone in Figure 1 consists of relatively old and compact rocks (pebblestone, limestone). The water table in the graben is very shallow, even at the surface at some locations. These geologic conditions significantly affected the distribution of damage observed in Dinar during the October 1, 1995 earthquake. Relatively less damage occurred in the mountain zone in comparison with serious damage occurred in the alluvial zone. The heaviest damage occurred in the transition zone separating these two areas (Erdik *et al.*, 1995).

In this study we used the aftershocks of the Dinar earthquake of October 1, 1995 recorded at 5 stations located in Dinar to estimate source parameters. Each station consists of a three components SSA-320 accelerometer and a GSR-16 recorder. The accelerometers have flat response between 0.1-20 Hz. Locations of the stations and epicenters of the 53 aftershocks are shown in Figure 2. The DSI station is located on the relatively compact Eocene aged limestone. The DDH station is located on the slope deposits in the transition zone and the DJK, DCE, DKH stations are located in the alluvial filled areas (Figure 1). Magnitudes and focal depths of the 53 aftershocks which were selected for this study range between M_L= 2.5 and M_L=4.1, h = 5 and 15 km respectively (KOERI, 1995).

METHOD AND DATA ANALYSIS

Method

The circular source model of Brune (1970) has been used in this study. Brune gave some simple relations between the source parameters of earthquakes and the spectral parameters (corner frequency, f_0, low frequency level, W_0, of S-wave displacement spectra) (Fig. 3). The seismic moment (M_0) is given by (Keilis-Borok, 1960):

$$M_0 = \frac{4\pi\rho R\beta^3\Omega_0}{kR_{\theta\phi}} \qquad (1)$$

where ρ is the density of the medium (gr/cm^3), β is the S-wave velocity (cm/sec), R is the source-station distance (cm), $R_{\theta\phi}$ is the radiation coefficient for S-wave, k is the free surface correction, and W_0 is the low frequency level on the spectra. In this study we adopted the values ρ = 2.6 gr/cm^3, β = 3.5 km/sec, $R_{\theta\phi}$ = 0.6 and k = 2 for the studied region.

The average low frequency level ($<W_0>$) which is normalized to hypocentral distance of 10 km is given by (Archuleta *et al.*, 1982):

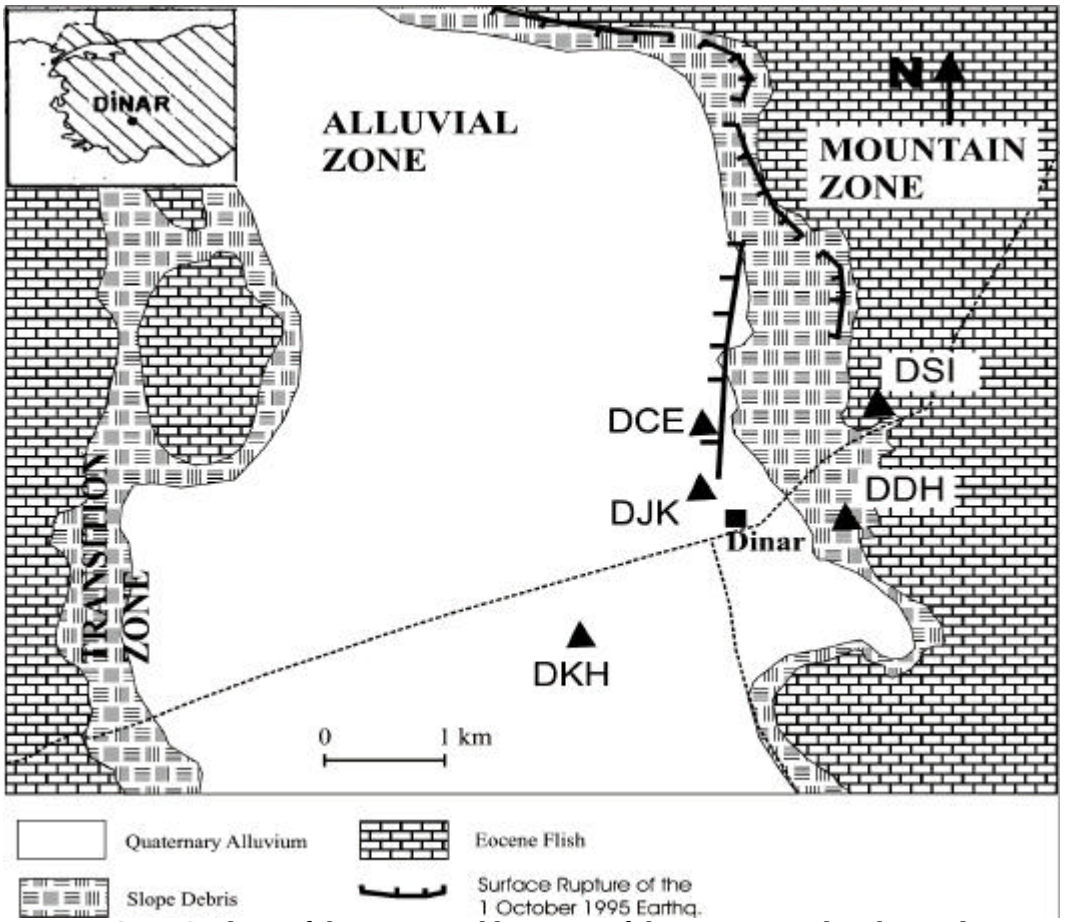

FIG. 1: Geology of the region and locations of the stations used in this study

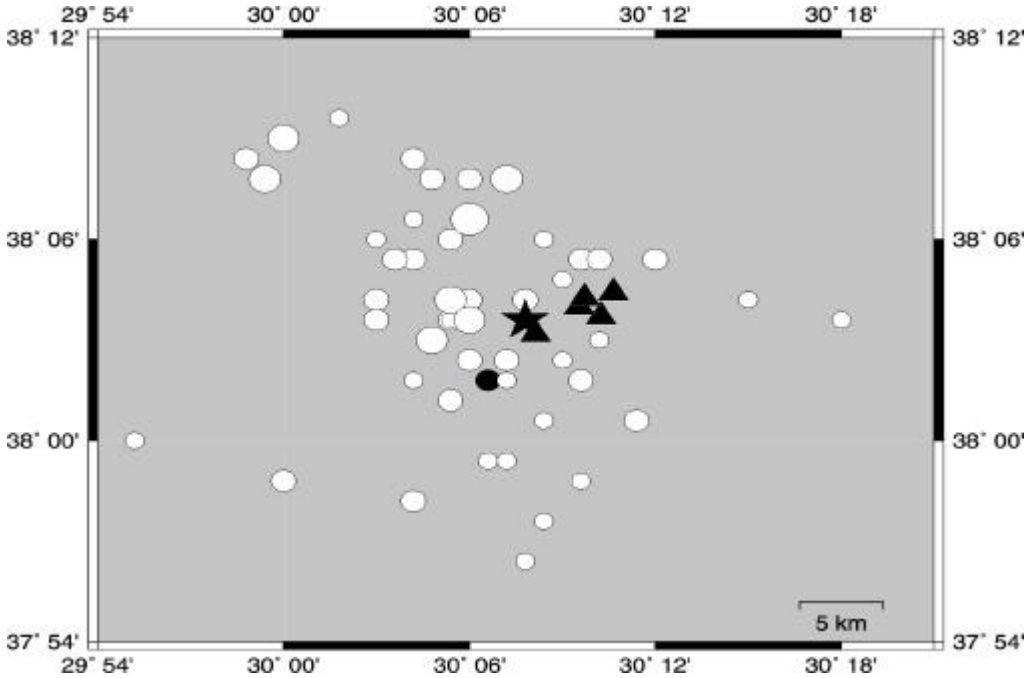

FIG. 2: Epicenters of the aftershocks of October 1, 1995 Dinar earthquake (circles) and locations of the stations (triangles) used in this study *(star and solid circle denote locations of the main shock and the event used in attenuation study respectively).*

$$<\Omega_0>=anti\log\left\{\frac{1}{NS}\sum_{i=1}^{NS}\log(\Omega_{0i}R_i/10)\right\} \quad (2)$$

where NS is the number of stations, R_i is the distance of station to focus, and W_{0i} is the low frequency level at each station. Similarly, the average seismic moment ($<M_0>$) can be calculated from (Archuleta *et al.*, 1982):

$$<M_0>=anti\log\left\{\frac{1}{NS}\sum_{i=1}^{NS}\log M_{0i}\right\} \quad (3)$$

where M_{0i} is the seismic moment computed at each station. The standard deviation and error are given by the following relations:

$$s.d.(\log<M_0>)=\left\{\frac{1}{NS-1}\sum_{i=1}^{NS}[\log M_{0i}-\log<M_0>]^2\right\}^{1/2} \quad (4)$$

and,

$$eM_0=anti\log\{s.d.(\log<M_0>)\} \quad (5)$$

Average corner frequency ($<f_0>$) and the error (ef_0) for corner frequency can be computed similarly.

The source radius for Brune's model is computed from:

$$r=\frac{2.34b}{2pf_0} \quad (6)$$

The average source radius ($<r>$) is computed from (Archuleta *et al.*, 1982):

$$<r>=\frac{1}{NS}\sum_{i=1}^{NS}r_i \quad (7)$$

The average stress drop ($<Ds>$) is computed by using the average seismic moment and the average source radius (Brune, 1970):

$$<\Delta s>=\frac{7<M_0>}{16<r>^3} \quad (8)$$

Data Analysis

To estimate the source parameters the part of SH waves of records are used after eliminating instrument effect. Firstly, for each event the transverse component was obtained from the horizontal components by using back azimuths. We selected the SH waves with a time window starting a short time before the S-wave arrival and lasting nearly 5 sec relative to decrease of energy from each transverse component (Fig. 3). This time window should be sufficiently long to detect the S-wave but should not allow to mix the other phases. An error of ±0.5 sec in window length does not change the shape of the spectrum significantly (Valdes-Gonzalez and Meyer, 1996).

By using the PITSA program (IASPEI, 1992) which applies the Trapezoidal Integration method the displacement records are computed from acceleration records. To keep the general characteristics of the signal unchanged a baseline correction is applied to the integrated signal. To avoid spectral complications arising from the use of rectangular time window a 10% effective cosine window has been applied to data before the Fast Fourier Transform (FFT).

After completing the above processing steps the data is transferred into the frequency domain by applying the FFT. Finally, for each event the spectral parameters, low frequency level (W_0) and corner frequency (f_0) are read from the displacement spectra visually. The spectral parameters read from the spectra, the source parameters and errors calculated by using the relations given above are listed along with the date, time, epicenter coordinates, and depth for the 53 aftershocks in Table 1.

RELATIONSHIPS AMONG SOURCE PARAMETERS

Relationships among the source parameters are important to understand the seismicity of a region. We plotted the seismic moment (M_0) versus the magnitude (M_L) for the 53 aftershocks in Figure 4. In the figure, while the open circles represent the values which are

calculated from single station, the solid circles represent the values which are calculated from two stations at least. As seen in Figure 4, the values determined from single station (open circles) do not fit the relation very well. To derive reliable W_0 from single station is very hard. Therefore, the values that are derived from single station recordings were not taken into account in further computations. A least squared best fitting line, which is shown with the solid line in the Figure 4, is given by:

$$\log M_0 = (1.19 \pm 0.14)\, M_L + (17.08 \pm 0.47) \quad (9)$$

where the correlation coefficient is 0.75.

The magnitude M_L is taken from the preliminary report of the October 1, 1995 Dinar earthquake (KOERI, 1995). This magnitude is not strictly a local magnitude M_L since it is not determined directly from Wood-Anderson seismographs. Therefore, we tested local magnitudes by correlating with moment magnitude, M_W, which can be calculated from seismic moment by using the formula proposed by Hanks and Kanamori (1979):

$$M_W = 2/3 \log M_0 + 10.7 \quad (10)$$

Moment magnitude versus local magnitude plot is shown in Figure 5. It is expected that $M_L \approx M_W$ for $M_W \leq 6.6$ (the dashed line in Figure 5) (e.g. Margaris and Papazachos, 1999). The equation of solid line in Figure 5 which represents the relation between M_L and M_W is:

$$M_W = 0.8\, M_L + 0.65 \quad (11)$$

where the correlation coefficient is 0.75.

This relation roughly fits the expected pattern. However, significant differences between M_L and M_W are seen toward high and low values, but at our magnitude range the error is relatively small.

As seen in Figure 4, our data fit the line quite well except for single station records (open circles), indicating that the magnitude is linearly related to the logarithm of seismic moment. M_0 versus M_L relationships show differences according to investigated region and magnitude range:

$\log M_0 = (1.07 \pm 0.16)\, M_L + (17.64 \pm 0.02)$
$0.5 \leq M_L \leq 3.5$ Petatlan-Mexico City (12)
(Valdes-Gonzalez and Meyer, 1996),

$\log M_0 = (1.21 \pm 0.03)\, M_L + (17.02 \pm 0.07)$
$0.0 \leq M_L \leq 6.0$ Oroville-California (13)
(Bakun and Lindh, 1977),

$\log M_0 = (1.20 \pm 0.05)\, M_L + (17.49 \pm 0.19)$
$1.0 \leq M_L \leq 6.0$ Mammoth Lakes California
(Chavez and Priestley, 1985) (14),

$\log M_0 = 1.5\, M_L + 16.07$
$3.9 \leq M_L \leq 6.6$ Greece (15)
(Margaris and Papazachos, 1999).

While the equation (9) we found is very similar to some of these relationships for example equations (13) and (14), it has greater and less slope than equation (12) and (15) respectively.

Kanamori and Anderson (1975) indicated that the stress drop is constant, independent of earthquake size. The importance of a constant stress drop for all earthquakes lies in the concept of similarity among earthquakes introduced by Aki (1967). The concept of similarity rests on two important assumptions: the stress drop is the same for all earthquakes, and the rupture velocity is the same for all earthquakes (Archuleta et al., 1982). In the other words, the shape of source spectrum changes with the size following a scaling law proposed by Aki (1967) that is $M_0 \propto f_0^{-3}$ or $M_0 \propto r^3$. Relationships among the seismic moment, source radius, and stress drop are shown in Figure 6. The relationship between seismic moment and source follows a steplike path that consists of the following three segments:

1. Earthquakes with seismic moment $M_0 >$ 1.0E+21 dyne.cm follow $M_0 \propto r^3$ as predicted by the seismic scaling law (Aki, 1967) (large ellipse in Figure 6). The corresponding average stress drop is 60 bars.
2. Earthquakes with $M_0 <$ 1.0E+21 dyne.cm follow $M_0 \propto r^{3.2}$ which the slope is some greater than the scaling slope (small ellipse in Figure 6). This shows that

stress drop decrease a small amount with decreasing seismic moment (approximately from 33 to 15 bars). But the average stress drop, 20 bars, is less 3 times than the first branch.

3. The branch consisting of earthquakes with M_0 from 4.0E+20 to 1.8E+21 dyne.cm which includes the bottom side of the first branch and the upper side of the second branch is almost vertical with a source radius of 200 m nearly (dashed ellipse in Figure 6). In this branch, the stress drop decrease approximately from 80 to 17 bars.

The direct implication of Figure 6 is the change of stress drop at nearly 1.0E+21dyne.cm. If we admit that the slight change in the slope relative to the scaling law for small earthquakes is within error limits, the stress drop is constant for each group. During the step of stress drops, source radius is constant at 200 m. Constant source radius outcome from constant corner frequency (equation 6). Variation of the corner frequency with seismic moment is shown in Figure 7. The Brune's model (1970) holds an inverse relationship between the source radius and corner frequency. It is expected that the corner frequency decreases with increasing magnitude. In Figure 7, stars show the expected corner frequencies, which are computed from $M_0 f_0^{-3} = constant$, along changing seismic moment. Figure 7 shows that the corner frequencies for earthquakes with M_0 < 1.0E+21 dyne.cm are not high as expected.

Decreasing stress drop with decreasing seismic moment and nearly constant corner frequency are investigated by many researchers (e.g. Archuleta *et al.*, 1982; Dysart *et al.*, 1988; Valdes-Gonzalez and Meyer, 1996; Jin *et al.*, 2000). Bakun *et al.* (1976), Tucker and Brune (1977), Rautian *et al.* (1978), and Chouet *et al.* (1978) have found the corner frequency independent of seismic moment for earthquakes of M < 3. It is an important problem whether the constant corner frequency for these earthquakes is due to constant source radius or to attenuation during propagation and local geology effect. Archuleta *et al.* (1982) have suggested two reasons for nearly constant source radius for earthquakes of $M_0 \leq$ 1.0E+21 dyne.cm. The first reason is the propagation effect (local geology effect or attenuation), the second reason is the length of the first rupture or distance between barriers. Iio (1986, 1992) has shown that source radius can not always be determined from the Brune's model. He suggested that microearthquakes (1.0E+10 < M_0 <1.0E+25) have relatively small rupture velocities and the rupture velocity increases with increasing rupture length. Frankel (1982) suggested that the corner frequencies of microearthquakes recorded at Virgin Islands are related to the ground conditions at seismometers locations. Andrews (1982) and Hanks (1982) found similar results.

THE EFFECT OF ATTENUATION AND LOCAL GEOLOGY

In estimating the source parameters of earthquakes, the removal of attenuation effect from the spectrum is important. This is possible in the case of having a good knowledge of attenuation for the studied area. We do not have a detailed attenuation study for the Dinar area. Therefore, we examined only the effect of attenuation on the spectral parameters (W_0 and f_0) for selected constant quality factor (Q_0) values. The spectrum was corrected for attenuation by multiplying it by the transfer function (Archuleta *et al.*, 1982);

$$e^{-pfR/Q_0 b} \qquad (16)$$

where f is the frequency (Hz), R is hypocenter distance (km), b is the S-wave velocity (km/sec), and Q_0 is the quality factor for S wave. For crustal rocks having S-wave velocity of 3.5 km/sec the value of Q_0 between 2-20 Hz is 200 or higher (Aki, 1980; Chouet *et al.*, 1978; Papageorgiou, 1981).

To study the attenuation effect in this study, we selected an aftershock of M_L=3.3 (10.10.95, 00:22:55) recorded at 5 stations, each station having a hypocentral distance of R≈11 km (solid circle in Figure 2). The DSI station is located in the mountain area where the surface layer consists of Eocene aged limestones. We selected a Q_0 = 400 for this station. The

DDH station is located in the transition zone consisting of continental sedimentary deposits and slope debris. Below these sediments the same rocks seen in the mountain area are continued. We selected a $Q_0 = 300$ for this station. The DJK, DCE, and DKH stations are located in the alluvial filled area. For these stations Q_0 values of 100, 200, and 100 were selected respectively. For the DKH station S-wave spectra before and after the removal of attenuation effect are shown in Figure 8. This result indicates that attenuation changes the spectra at only high frequencies, however this does not affect the spectral parameters (W_0 and f_0) significantly. Since the results for other stations are similar they are not shown here.

Separately, in this study we examined the spectra of the same earthquake (10.10.95, 04:14:42) recorded at different stations and the spectra of the earthquakes with different magnitudes recorded at the same station (DDH) (Figures 9 and 10 respectively). Because the distances between the stations are small, the corner frequency, which is related to source dimension, should be same at all stations for the same earthquake. But, as seen in Figure 9, the corner frequencies are not same at all stations, because the local geology underlying the stations is different. On the other hand, the corner frequency is expected to change with changing magnitude. But, as seen in Figure 10, the corner frequencies are nearly constant at DDH station, for earthquakes having magnitudes from 2.5 to 3.6. Therefore, it can be stated that corner frequency is significantly affected from local geology of underlying stations

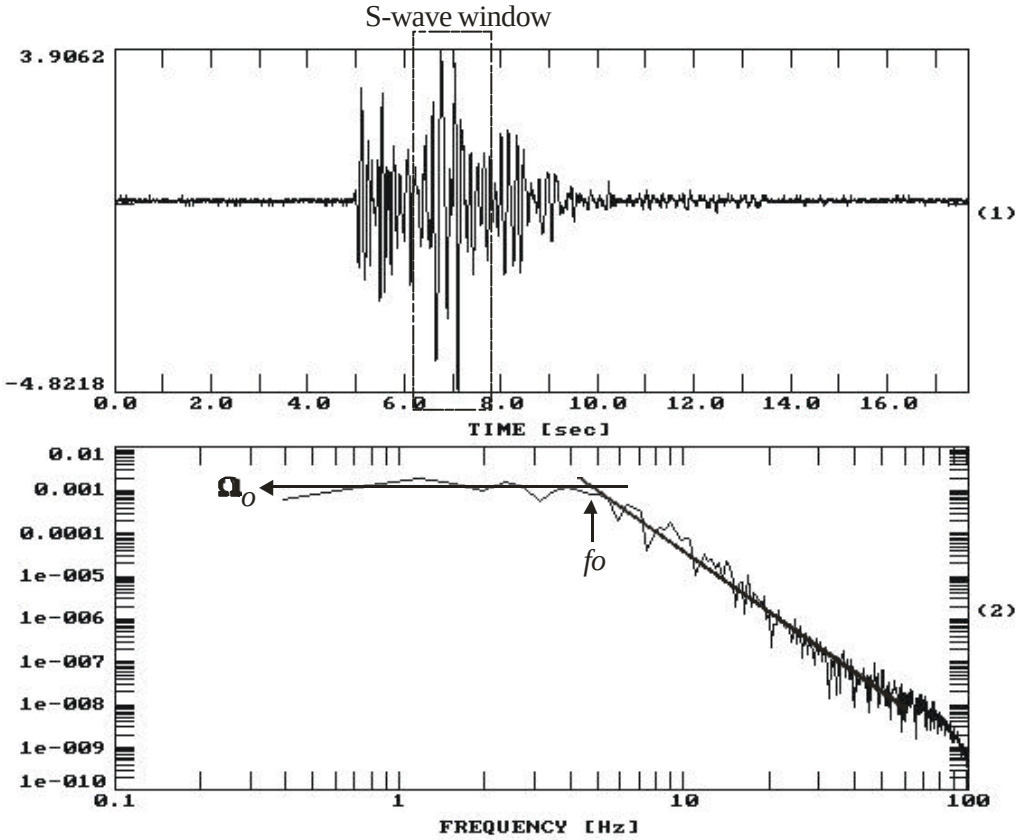

FIG. 3: S-wave window (above) and its displacement spectrum (below). W_0 ; the low frequency level, f_0 ; the corner frequency.

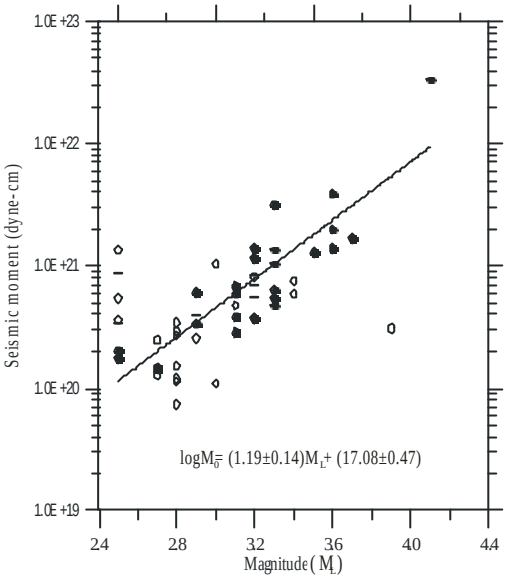

FIG. 4: The seismic moment versus the local magnitude. Filled symbols represent averaged values of more than one station records and open symbols represent single station record (*a least squared best fitting line represents only the data recorded by two stations at least).*

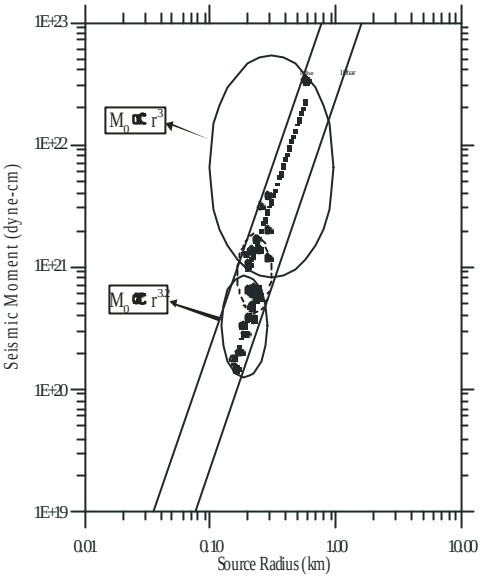

FIG. 6: The seismic moment versus the source radius. The solid lines represent constant stress drop.

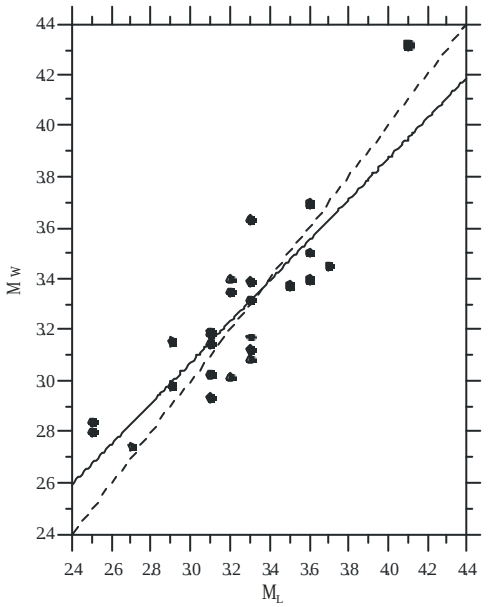

FIG. 5: Relationship between the local magnitude (M_L) and the moment magnitude (M_W) for data recorded by two stations at least. Dashed line and continuous line represent the relations of $M_L=M_W$ and

$M_W = 0.8\ M_L + 0.65$ respectively.

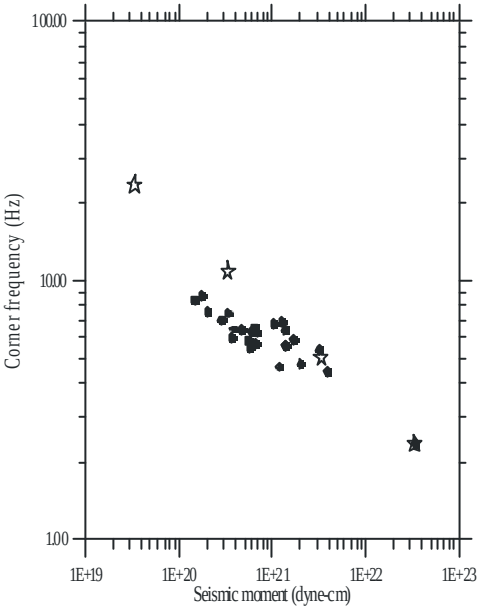

FIG. 7: The corner frequency versus the seismic moment. Stars show changing of the corner frequencies relative to

$M_0\ f_0^{-3} = constant.$

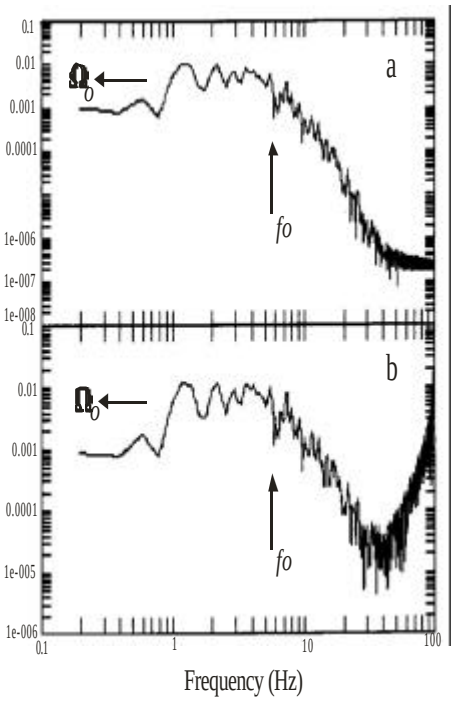

FIG. 8: The amplitude spectrum of an earthquake (M_L=3.3, 10.10.95, 00:22:55) recorded at the DKH station, before (a) and after (b) the attenuation effect was removed.

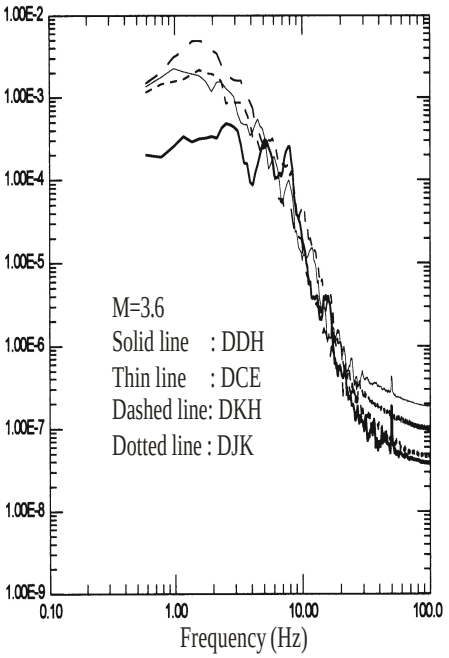

FIG. 9: The spectra of the same earthquake (10.10.95, 04:14:42) recorded at different stations.

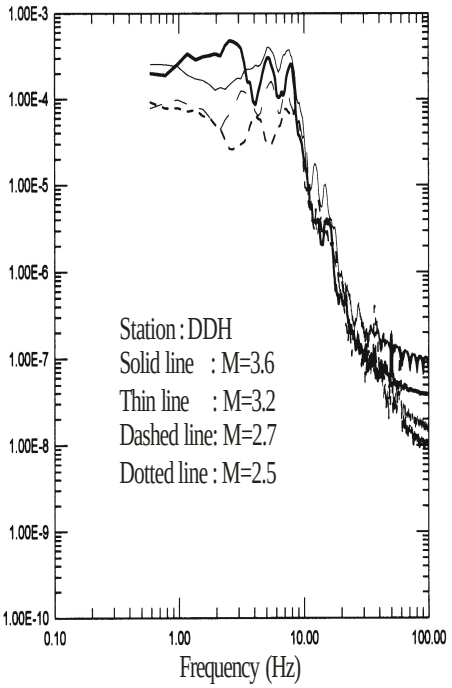

FIG. 10: The spectra of different earthquakes recorded at the same station (DDH).

Table 1. Spectral and source parameters of studied earthquakes.

N	Date	Time	Lat.	Long.	h	M_L	$<\Omega_0>$	$\Omega\varepsilon_0$	$<f_0>$	$\varepsilon\phi_0$	$<M_0>$	εM_0	<r>	$<\Delta\sigma>$	NS
1	07.10.95	17:26:58	38.14	29.98	10	3.2	3.21E-04		7		3.75E+20		0.19	25.39	1
2	07.10.95	18:17:57	38.13	30.1	10	3.4	5.00E-04		7		5.84E+20		0.19	39.59	1
3	08.10.95	2:18:19	38.07	30.05	8	3.4	6.50E-04		7.2		7.59E+20		0.18	55.95	1
4	08.10.95	3:36:01	38.11	30.07	10	2.8	1.31E-04		8.2		1.52E+20		0.16	16.59	1
5	08.10.95	3:50:49	38.05	30.08	10	3.9	2.62E-04		8		3.06E+20		0.16	30.93	1
6	08.10.95	3:52:15	37.97	30.07	9	3.1	4.05E-04		7.8		4.73E+20		0.17	44.32	1
7	08.10.95	4:26:46	38.06	30.09	10	3.2	7.26E-04		7.2		8.48E+20		0.18	62.49	1
8	08.10.95	11:05:41	38.03	30.11	10	3	9.44E-05		8.2		1.10E+20		0.16	12	1
9	08.10.95	21:26:49	38.09	30.07	5	3.3	4.04E-04	2.07	6.45	1.4	4.72E+20	1.82	0.21	23.33	2
10	08.10.95	22:00:32	38.13	30.08	7	3.3	5.48E-04	2.33	6.57	1.4	6.39E+20	2.11	0.2	33.01	2
11	08.10.95	22:42:12	38.07	30.25	10	2.9	2.82E-04		5.8		3.29E+20		0.22	12.69	1
12	08.10.95	23:08:21	38.07	30.1	10	3.1	3.29E-04	1.31	6.52	1.2	3.85E+20	1.19	0.2	20.17	3
13	08.10.95	23:39:59	38.13	29.99	10	3.6	1.19E-03	3.11	5.65	1.4	1.39E+21	2.15	0.24	44.57	3
14	08.10.95	23:56:25	37.96	30.14	12	2.7	1.13E-04		8		1.32E+20		0.16	13.39	1
15	09.10.95	0:16:49	38.02	30.09	10	3.1	5.67E-04	2.32	5.73	1.3	6.62E+20	2.16	0.23	22.99	3
16	09.10.95	0:55:32	38.07	30.13	10	3.3	4.65E-04	1.24	5.86	1.4	5.43E+20	1.21	0.23	19.47	3
17	09.10.95	5:40:35	38.06	30.05	10	3	8.82E-04		5.8		1.03E+21		0.22	39.68	1
18	09.10.95	6:16:20	38.03	30.12	15	2.5	7.44E-04		7		8.69E+20		0.19	58.85	1
19	09.10.95	6:43:04	38.04	30.1	11	3.3	8.98E-04	2.46	6.84	1.3	1.05E+21	2.25	0.2	61.37	3
20	09.10.95	10:34:14	38.15	30	5	3.6	3.33E-03	2.06	4.47	1.2	3.89E+21	1.02	0.29	67.41	2
21	09.10.95	11:41:50	38	29.92	10	2.9	2.22E-04		6.6		2.59E+20		0.2	14.72	1
22	09.10.95	13:52:11	37.98	30	10	3.2	6.96E-04		6		8.12E+20		0.22	34.67	1
23	09.10.95	17:50:50	38.09	30.06	10	3.2	1.01E-03	2.61	4.66	1.3	1.17E+21	2.36	0.29	21.71	4
24	09.10.95	18:10:26	37.94	30.13	15	2.5	2.89E-04		7.6		3.38E+20		0.17	29.31	1
25	09.10.95	18:34:33	38.1	30.14	10	2.5	1.73E-04	1.48	7.6	1.2	2.02E+20	1.46	0.17	17.18	2
26	09.10.95	18:40:00	38.14	29.88	10	2.5	1.16E-03		7.2		1.36E+21		0.18	100.1	1
27	09.10.95	19:44:05	38.06	30.09	15	2.5	3.12E-04		7		3.64E+20		0.19	24.68	1
28	09.10.95	21:37:02	38.03	30.16	10	3.2	3.19E-04	1.45	6.04	1.3	3.72E+20	1.46	0.22	15.25	3
29	09.10.95	22:16:55	38.16	30.03	10	2.5	4.63E-04		7.1		5.40E+20		0.18	38.2	1
30	10.10.95	0:22:55	38.04	30.12	10	3.3	2.68E-03	2.9	5.42	1.3	3.13E+21	2.79	0.25	91.74	5
31	10.10.95	2:01:33	37.99	30.12	10	2.8	9.84E-05		8		1.15E+20		0.16	11.62	1
32	10.10.95	3:38:44	38.1	30.09	10	3.2	4.76E-04		5		5.56E+20		0.26	13.72	1
33	10.10.95	4:14:42	38.13	30.12	6	3.6	1.71E-03	2.39	4.74	1.4	2.00E+21	2.31	0.29	36.94	4
34	10.10.95	5:47:17	38.14	30.07	10	3.2	6.00E-04		5.5		7.00E+20		0.24	23.02	1
35	10.10.95	5:59:11	38.06	30.3	10	2.9	3.40E-04		7.2		3.97E+20		0.18	29.26	1
36	10.10.95	8:28:49	38.05	30.17	10	2.8	1.03E-04		6		1.20E+20		0.22	5.13	1
37	10.10.95	8:56:31	38.08	30.15	10	2.8	6.30E-05		8.2		7.35E+19		0.16	8.01	1
38	10.10.95	10:36:43	38.03	30.07	13	2.8	2.90E-04		6		3.39E+20		0.22	14.45	1
39	10.10.95	13:25:43	37.99	30.11	15	2.8	2.53E-04		8.5		2.96E+20		0.15	35.9	1
40	10.10.95	17:24:31	38.09	30.16	14	3.3	1.18E-03	2.37	6.42	1.3	1.37E+21	2.02	0.21	69.36	2
41	10.10.95	17:33:53	38.01	30.19	10	3.2	1.20E-03	1.91	5.65	1.4	1.40E+21	1.89	0.24	45.44	3
42	10.10.95	18:18:12	37.98	30.16	10	2.8	2.34E-04		6.5		2.73E+20		0.2	14.82	1
43	11.10.95	0:07:43	38.09	30.2	10	3.1	2.44E-04	1.83	7.01	1.3	2.85E+20	1.81	0.19	18.72	2
44	11.10.95	1:13:16	38.09	30.17	10	2.9	2.85E-04	1.59	7.47	1.3	3.32E+20	1.58	0.18	25.87	4
45	11.10.95	2:26:09	38.04	30.15	11	2.9	5.17E-04	1.79	6.34	1.4	6.04E+20	1.74	0.21	27.52	4
46	11.10.95	5:48:52	38.06	30.1	10	2.7	2.14E-04		6.8		2.50E+20		0.19	15.52	1
47	11.10.95	6:44:58	38.11	30.1	10	4.1	2.87E-02	7.7	2.34	1.2	3.35E+22	7.43	0.57	81.15	5
48	11.10.95	8:40:20	38.09	30.17	10	3.1	5.89E-04	1.88	6.29	1.4	6.87E+20	1.89	0.22	30.08	4
49	11.10.95	17:12:51	38.07	30.1	7	3.1	4.99E-04	2.34	5.48	1.3	5.82E+20	2.15	0.24	17.4	4
50	11.10.95	17:59:55	38.1	30.15	10	2.7	1.25E-04	1.42	8.39	1.1	1.46E+20	1.39	0.16	16.99	2
51	12.10.95	2:28:45	38.07	30.09	10	3.5	1.10E-03	2.53	6.93	1.2	1.28E+21	2.27	0.19	81.67	2
52	12.10.95	3:07:14	38.01	30.14	13	2.5	1.51E-04	2.71	8.75	1	1.77E+20	2.34	0.15	23.32	2
53	12.10.95	8:30:17	38.06	30.1	5	3.7	1.43E-03	2.8	5.9	1.3	1.67E+21	2.32	0.23	62.09	4

In Table 1 **:** *N* is the event number, *Date* (day.month.year), *Time* is UT (hour :minute:second), *h* is the focal depth of the earthquake (km), M_L is the local magnitude, $<W_0>$ is the average low frequency level normalized to 10 km (cm.sec), eW_0 is the multiplicative error factor for Ω_0, $<f_0>$ is the average corner frequency (Hz), ef_0 is the multiplicative error factor for f_0, $<M_0>$ is the average seismic moment (dyne.cm), eM_0 is the multiplicative error factor for M_0, $<r>$ is the average source radius (km), $<Ds>$ is the average stress drop (bar), *NS* is the number of stations used to determine source parameters.

CONCLUSIONS

Source parameters of 53 aftershocks of the Dinar earthquake of October 1, 1995 have been estimated from the S-wave displacement spectra by using the circular source model of Brune (1970). A linear relationship between the magnitude M_L and seismic moment M_0 has been determined by using two stations records at least:

$$\log M_0 = (1.19 \pm 0.14) M_L + (17.08 \pm 0.47) \quad (17)$$

From the relationships among the seismic moment, the source radius, and the stress drop it is seen that the stress drop shows a step near to the moment of 1.0E+21 dyne.cm corresponding to a source radius of 200 m. Different stress drops for small and mid-large earthquakes may be resulting from the bandlimited fractal nature of fault zones or the barrier effect (Jin *et al.*, 2000).

S-wave spectra are affected from the attenuation only at high frequencies, and this does not alter the source parameters estimations. Corner frequencies were significantly affected from the local geology of instrument locations. Therefore, the correct scaling law needs the knowledge of local geology effect.

ACKNOWLEDGMENTS

The authors would like to thank E.M. Scordilis and Vassilis Karakostas for their critical reviews. This work was supported by the Research Found of the Istanbul University. Project number: 1176/070998, B-42/180998.

REFERENCES

Aki, K., 1967, Scaling law of seismic spectrum: J. Geophys. Res., **72**, 1217-1231.

Aki, K., 1980, Attenuation of shear-waves in the litosphere for frequencies from 0.05 to 25 Hz: Phys. Earth. Planet Inter., **21**, 50-60.

Andrews, D. J., 1982, Separation of source and propagation spectra of seven Mammoth Lakes aftershocks: in Proc. Workshop XVI, Dynamic Characteristics of Faulting, 1981, U.S. Geol. Surv., Open-File Rep., **82-591**, 437-454.

Archuleta, R. J., Cranswick, E., Mueller, C., and Spudich, P., 1982, Source parameters of the 1980 Mammoth Lakes, California earthquake sequence: J. Geophys. Res., **87**, 4595-4607.

Bakun, W. H., Bufe, C. G., and Stewart, R. M., 1976, Body-wave spectra of central California earthquakes: Bull. Seism. Soc. Am., **66**, 363-384.

Bakun, W. H., and Lindh, A. G., 1977, Local magnitudes, seismic moments, and coda durations for earthquakes near Oroville, California: Bull. Seism. Soc. Am., **67**, 615-629.

Biçmen, F., 1992, Marmara bölgesindeki yerel depremlerin kaynak parametrelerinin belirlenmesi: Yüksek Lisans Tezi, Ý.Ü. Fen Bil. Enst.

Brune, J. N., 1970, Tectonic stress and the spectra of seismic shear waves from earthquakes: J. Geophys. Res., **75**, 4997-5009.

Chavez, D. E., and Priestley, K. F., 1985, M_L observations in the Great Basin and M_0 versus M_L relationships for the 1980 Mammoth Lakes, California,

earthquake sequence: Bull. Seism. Soc. Am., **75**, 1583-1598.

Chouet, B., Aki, K., and Tsujiura, M., 1978, Regional variation of the scaling law of earthquake source spectra: Bull. Seism. Soc. Am., **68**, 49-79.

Dysart, P. S., Snake, J. A., Sacks, I. S., 1988, Source parameters and scaling relations for small earthquakes in the Matsushiro region, southwest Honshu, Japan: Bull. Seism. Soc. Am., **78**, 571-589.

Erdik, M., Aydinoðlu, M. N., Pýnar, A., ve Kalafat, D., 1995, 1 Ekim 1995 Dinar depremi (Ms=6.1) ön inceleme raporu: TMMOB Ýnþaat Mühendisleri Odasý Aylýk yayýn Organý, Sayý 24.

Fletcher, J. B., 1980, Spectra from high dynamic range digital recordings of Oroville, California aftershocks and their source parameters: Bull. Seism. Soc. Am., **70**, 735-755.

Frankel, A., 1982, The effects of attenuation and site response on the spectra of microearthquakes in the northeastern Caribbean: Bull. Seism. Soc. Am., **72**, 1379-1402.

Frankel, A., and Wennerberg, L., 1989, Microearthquake spectra from the Anza, California, seismic network: site response and source scaling: Bull. Seism. Soc. Am., **79**, 581-609.

Hanks, T. C., and Kanamori, H., 1979, A moment magnitude scale: J. Geophys. Res., **84**, 2348-2350.

Hanks, T. C., 1982, f_{max}: Bull. Seism. Soc. Am., **72**, 1869-1879.

IASPEI, 1992, Programmable interactive toolbox for seismological analysis (PITSA): Scherbaum, F., and Johnson, J. (edt.), IASPEI Software Library 5.

Iio, Y., 1986, Scaling relation between earthquake size and duration of faulting for shallow earthquakes in seismic moment between 10^{10} and 10^{25} dyne.cm: J. Phys. Earth, **34**, 127-169.

Iio, Y., 1992, Seismic source spectrum of microearthquakes: Bull. Seism. Soc. Am., **82**, 2391-2409.

Ishida, M., and Kanamori, H., 1980, Temporal variation of seismicity and spectrum of small earthquakes preceding the 1952 Kern County, California, earthquake: Bull. Seism. Soc. Am., **70**, 509-527.

Jin, A., Moya, C. A., and Ando, M., 2000, Simultaneous determination of site responses and source parameters of small earthquakes along the Atotsugawa fault zone, central Japan: Bull. Seism. Soc. Am., **90**, 1430-1445.

Kanamori, H., and Anderson, D.L., 1975, Theoretical basis for some empirical relation in seismology: Bull. Seism. Soc. Am., **65**, 1073-1095.

Kaypak, B., 1995, 13 Mart 1992 Erzincan depremi artsarsýntýlarý kaynak parametreleri: Yüksek Lisans Tezi, Ý.T.Ü. Fen Bil. Enst.

Keilis-Borok, V. I., 1960, Investigation of the mechanism of earthquakes: Sov. Res. Geophys., (English transl.), **4**, 29.

Koçyiðit, A., 1984, Güneybatý ve yakýn dolayýnda levha içi yeni tektonik geliºim: TJKB, **27**, 1-16.

KOERI, 1995, 1 Ekim 1995 Dinar depremi ve artçý þoklarý: B.Ü. Kandilli Rasathanesi ve Deprem Araþtýrma Enstitüsü, Sismoloji Lab., Ýstanbul.

Mandal, P., Rastogi, B. K., and Sarma, C. S. P., 1998, Source parameters of Koyna earthquakes, India: Bull. Seism. Soc. Am., **88**, 833-842.

Margaris, B. N., and Papazachos, C. B., 1999, Moment-magnitude relations based on strong-motion records in Greece: Bull. Seism. Soc. Am., **89**, 442-455.

Öncel, A. O., Koral, H., and Alptekin, Ö., 1998, The Dinar earthquake (Mw=6.2; October 1, 1995; Afyon-Turkey) and earthquake hazard of the Dinar-Çivril fault: Pure and Appl. Geophys., **152**, 91-105.

Papageorgiou, A. S., 1981, On an earthquake source model of inhomogeneous faulting and its application to earthquake engineering: Ph.D. dissertion, Mass. Inst. of Technol., Cambridge.

Polat, O., 1995, Bursa ve çevresindeki küçük depremlerin ivme kayýtlarýnýn incelenmesi: Yüksek Lisan Tezi, Ý.T.Ü. Fen Bil. Enst.

Rautian, T. G., Khalturin, V. I., Martinov, V. G., and Molnar, P., 1978, Preliminary analysis of the spectral content of P and S waves from local earthquakes in the Garm, Tadjikistan

region: Bull. Seism. Soc. Am., **68**, 949-972.

Tucker, B. E., and Brune, J. N., 1977, Source mechanism and M_b-M_s analysis of aftershocks of the San Fernando earthquake: Geophys. J. R. Astr. Soc. Am., **49**, 371-426.

Utkucu, M., Pýnar, A., and Alptekin, Ö., 2002, A detailed slip model for the 1995, October 1, Dinar, Turkey, earthquake (Ms=6.1) determined from inversion of teleseismic P and SH waveforms: Geophysical Journal International, **151**, 184-195.

Valdes-Gonzalez, C., and Meyer, R. P., 1996, Spectral analysis and earthquake scaling of the Petatlan earthquake (M_s=7.6) aftershocks, recorded at stations along the Pacific Coast and between the Coast and Mexico City: Pure and Appl. Geophys., **147**, 631-656.

Filename: Yalcinkaya_1_mike_1.doc
Directory: C:\BGSJournal\BGS_2_2003\Final
Template: C:\WINDOWS\Application Data\Microsoft\Templates\Normal.dot
Title: Relationships among source parameters of aftershocks of the October 1, 1995 Dinar (Turkey) earthquake
Subject:
Author: mitica
Keywords:
Comments:
Creation Date: 01.06.2001 10:20
Change Number: 4
Last Saved On: 01.06.2001 11:26
Last Saved By: mitica
Total Editing Time: 22 Minutes
Last Printed On: 29.03.2004 12:37
As of Last Complete Printing
Number of Pages: 13
Number of Words: 4,923 (approx.)
Number of Characters: 28,557 (approx.)